




Efficacy of *Larimichthys crocea* TASOR protein-derived peptide FAM286 against *Staphylococcus aureus*

Ritian Jin, Guanglei Wei, Rong Lin, Wenfeng Lin, Jude Juventus Aweya, Duo Liang, Wuyin Weng, Shen Yang^{*} 

College of Ocean Food and Biological Engineering, Fujian Provincial Key Laboratory of Food Microbiology and Enzyme Engineering, Jimei University, Xiamen, Fujian, 361021, China

ARTICLE INFO

Keywords:

Staphylococcus aureus
Antimicrobial peptide
Larimichthys crocea
TASOR protein
Antimicrobial mechanism

ABSTRACT

Staphylococcus aureus (*S. aureus*) is a major foodborne pathogen, could lead cause of intestinal infections in humans. Antimicrobial peptides, as emerging antimicrobial agents, are gradually replacing traditional agents due to their highly effective and safe antimicrobial activity. In this study, a novel peptide, designated as FAM286, was identified from TASOR protein of *Larimichthys crocea*, which had a strong antimicrobial activity against *S. aureus* with a minimum bactericidal concentration (MBC) of 3.9 µg/mL and completed bacteria killing by treatment for 1.5 h. The FAM286 could increase the permeability and disrupt the integrity of cell membranes. The cell showed aggregation phenomenon and entered the apoptosis stage. In addition, the non-bactericidal concentration of FAM286 could effectively inhibit the formation of biofilm and remove mature biofilm. Molecular docking experiments further verified the binding sites of FAM286 to *S. aureus* biofilm proteins SarA, AgrA, and Hld. FAM286 could also bind the bacterial DNA in an embedded manner, disrupting the structure of DNA and leading to the death of bacteria. This study comprehensively evaluated the antimicrobial mechanism of the FAM286 against *S. aureus* and provided a theoretical basis for the prevention and control of *S. aureus*.

1. Introduction

Foodborne diseases are a widely followed health issue worldwide (Kumar et al., 2023). *Staphylococcus aureus* (*S. aureus*) as a major foodborne pathogen, can contaminate food during food preparation and processing, resulting in food poisoning (Bencardino et al., 2021). Statistical analysis of 165 strains of *S. aureus* isolated from 95 food poisoning events from 2006 to 2019 revealed that 90.30% of the strains carried genes for high-risk toxins that can cause food poisoning (Wan et al., 2023). To prevent such incidents, chemically synthesized preservatives are commonly used in the food industry, posing certain safety risks to human health (Erickson and Doyle, 2017). Furthermore, the increasing misuse of antibiotics has led to the emergence of drug resistance in pathogenic bacteria, which in turn has heightened the health risks posed by these bacteria to the food industry (Larsen et al., 2016). Therefore, it has become an important and urgent task to explore natural products with high antimicrobial activity to reduce the reliance of chemically synthesized preservatives.

Antimicrobial peptides (AMPs) have received widespread attention

for their efficient, safe and residue-free bactericidal activity as a potential alternative to antibiotics and preservatives, and have broad application prospects in the food industry (Tkaczewska, 2020). Most AMPs adsorb to the cell membrane of bacteria through electrostatic and hydrophobic interactions, causing physical damage to the membrane through direct action on the membrane, or entering the interior of the cell to act on DNA and proteins to exert antimicrobial activity (S. Li et al., 2021). Their non-specific mechanisms do not involve binding to specific targets, which making it difficult for bacteria to develop resistance. These mechanisms are distinct from the antibiotic inhibition mechanisms, which often act as inhibition by interfering with the metabolic processes of pathogenic microorganisms (Browne et al., 2020). AMPs constitute an important part of the non-specific immune system of fish, and serve as the first line of defense against various pathogens (Liu et al., 2023; Wang et al., 2022). Studies have shown that *Larimichthys crocea* (*L. crocea*) has a well-developed innate immune system (Liu et al., 2017; Wu et al., 2014). After being infected by bacteria, the expression of many innate immune-related AMPs such as Hepcidins (Zhang et al., 2021), Piscidins (Zheng et al., 2018) and

^{*} Corresponding author. College of Ocean Food and Biological Engineering, Jimei University, Xiamen, Fujian, 361021, China.

E-mail address: yangshen@jmu.edu.cn (S. Yang).

<https://doi.org/10.1016/j.crf.2025.100998>

Received 22 September 2024; Received in revised form 22 January 2025; Accepted 3 February 2025

Available online 3 February 2025

2665-9271/© 2025 The Authors. Published by Elsevier B.V. This is an open access article under the CC BY-NC license (<http://creativecommons.org/licenses/by-nc/4.0/>).

β -Defensins (K. Li et al., 2021) was up-regulated, playing crucial roles in the defense against bacteria in *L. crocea*. Therefore, *L. crocea* is one of the promising sources for isolation and identification of AMPs.

In this study, we used ultra-performance liquid chromatography-mass spectrometry (UPLC-MS) to search for peptide fragments with antimicrobial activity and elucidated the mechanism by which they inhibit *S. aureus* in an attempt to provide theoretical basis for the invention of natural antimicrobial agents derived from *L. crocea*.

2. Materials and methods

2.1. Materials and reagents

L. crocea was obtained from Ningde City, Fujian Province, China. Commercial *Staphylococcus aureus* (ATCC 12600) were obtained from the American Type Culture Collection. Nutrient Broth (NB) medium, Luria-Bertani (LB) medium was purchased from Huankai Microbial Technology (Guangzhou, Guangdong, China), and agar was purchased from LabLead Co., Ltd (Beijing, China). ϵ -Polylysine was purchased from Xinyinxiang Biological Engineering Co. (Zhejiang, China). Enrofloxacin, norfloxacin, amoxicillin, florfenicol were purchased from Yuanye Biotechnology Co. (Shanghai, China). Nisin (900 IU/mg) was purchased from Macklin Biochemical Technology Co. (Shanghai, China). TIANamp Bacteria DNA Kit (DP302) was purchased from Tiangen Biochemical Technology Co. (Beijing, China). Ethidium bromide (EB) dye was purchased from West Asia Reagent (Chengdu, Sichuan, China). Kanamycin, propidium iodide (PI) dye, nucleic acid dye, $10 \times$ DNA loading buffer, and ANNEXIN V-FITC/PI Apoptosis Assay Kit were purchased from Solarbio Technology Co. (Beijing, China).

2.2. Screening and synthesis of AMPs

200g of *L. crocea* were crushed with appropriate amount of ultrapure water for 3–5 min, and centrifuged at $1250 \times g$ for 20 min. And the supernatant was passed through a 3000 Da filter membrane and stored at -20°C for further analysis. The peptide sequences in the supernatant of *L. crocea* were analyzed by ultra-performance liquid chromatography-mass spectrometry (UPLC-MS) using a C18 analytical column with a length of 25 cm and an inner diameter of $75 \mu\text{m}$, and the mobile phase A was 0.1% aqueous methanol, and the mobile phase B was acetonitrile. The sample was injected into 5 mL for gradient elution in ultra-high performance liquid chromatography. The mass spectrometry conditions were set as gas flow rate: 40 mL/min, auxiliary gas rate: 10 mL/min, spray voltage: 3.0 kV, capillary temperature: 300°C , S-lens: 50%, HCD: 27%. Scan mode was positive ion, Full ms dd-MS2, primary scan: resolution 70,000, range 350–1600 m/z, secondary scan: resolution 17,500, fixed first mass 120 m/z. Dynamic exclusion: 10.0 s. The peptide information was obtained by searching the database using MAXQUANT (v1.6.5.0) software: *Larimichthys crocea* (Large yellow croaker) (Yang et al., 2023).

The hydrophobic ratio and net charge of the resulting peptides were calculated using the online software APD3 (Antimicrobial Peptide Database 3), and peptides matching the properties of the AMPs were screened. The 3D structure of FAM286 was predicted by Swiss-Model software, and the resulting tertiary structure was edited and processed by Pymol 2.0 software. The peptide was synthesized and purified by a commercial company, Scilight Biotechnology Co. Peptides were purified to more than 99% purity using HPLC with an Agela C18 column. The purity and molecular mass of the purified synthetic peptides were determined by liquid chromatography coupled to mass spectrometry (LC-MS/ESI) (Yang et al., 2021).

2.3. Determination of antimicrobial activity

2.3.1. Determination of the minimum bactericidal concentration (MBC)

The MBC of the peptide FAM286 against *S. aureus* was verified by the

plate colony counting method as described with some modifications (Tao et al., 2025). *S. aureus* suspension was cultured in 20 mL NB medium at 37°C for 8 h to logarithmic growth phase, and subsequently diluted to a concentration of 10^{5-6} CFU/mL with sterile PBS (0.01 M, pH 7.2). Peptide FAM286 was first dissolved in sterile PBS, which was followed by adding an equal volume of the bacterial suspension, and then the mixture was cultured for 2 h at 37°C . An equal amount of sterile PBS was used as a negative control. 20 μL of the samples were spread on glass petri dishes and incubated at 37°C for 24 h for colony counting. Additionally, four common antibiotics (amoxicillin, kanamycin, enrofloxacin, florfenicol) and food preservatives (ϵ -polylysine, nisin) were selected for comparison. The MBC was determined as the lowest concentration of the sample at which no bacterial growth was observed on the agar plate after the incubation period.

2.3.2. Time-kill curve analysis of FAM286

S. aureus was cultured to logarithmic growth phase and diluted to 10^{5-6} CFU/mL, and an equal volume of FAM286 was added to the bacterial solution to a final concentration of $1 \times$ MBC, $2 \times$ MBC and $4 \times$ MBC, and then incubated at 37°C . An equal volume of sterile PBS (0.01 M, pH 7.2) was used to culture with bacteria suspensions as negative control, kanamycin and ϵ -polylysine as positive controls. Next, 20 μL of the samples were spread on glass petri dishes at 0, 0.5, 1, 1.5, 2, 2.5 and 3 h. The colonies were counted after culture on NB plates at 37°C for 24 h (Weng et al., 2023).

2.4. Antimicrobial mechanism of peptide FAM286 against *S. aureus*

2.4.1. Effect on cell membrane permeability

The antimicrobial activity of the FAM286 was determined according to the method described previously with some modifications (Ashrafudoulla et al., 2020). *S. aureus* suspension cultured to logarithmic growth phase was taken and 1 mL was centrifuged at $6750 \times g$ for 1 min. Then the bacterial precipitate was washed three times with sterile PBS (0.01 M pH 7.2) and the concentration of the suspension was diluted to 10^{5-6} CFU/mL. An equal volume of FAM286 was mixed with the bacterial solution to achieve final concentrations of $1 \times$ MBC, $2 \times$ MBC, $4 \times$ MBC. An equal volume of sterile PBS (0.01 M pH 7.2) was used as the negative control, kanamycin and ϵ -polylysine as positive controls. Incubation was performed at 37°C and absorbance at 260 nm and 280 nm was measured every 1 h using a multimode plate reader.

2.4.2. Transmission electron microscopy (TEM)

S. aureus in the logarithmic growth stage was diluted to 10^{5-6} CFU/mL, and an equal proportion of $1 \times$ MBC FAM286 was added and incubated at 37°C for 2 h. An equal amount of sterile PBS (0.01 M, pH 7.2) was used as a control. The precipitate was collected by centrifugation at $6750 \times g$ for 1 min and washed three times with PBS. And double fixed with 2.5% glutaraldehyde and 1% osmic acid solution, and dehydrated with graded concentrations (30%, 50%, 70%, 80%) of ethanol solution, each concentration was treated for 15 min, and thereafter, transitioned to 90% and 95% acetone solution, respectively, treated for 15 min. Finally, treated with pure acetone twice, each time for 20 min. And after that, it was heated at 70°C for overnight embedding. Sections of 70–90 nm were obtained on copper grids. The slices were stained with uranyl acetate and lead citrate for 8–10 min, dried and then visualized by transmission electron microscopy (Yang et al., 2020a).

2.4.3. Effect on cell membrane integrity

1 mL of *S. aureus*, cultured in LB broth to logarithmic growth phase, was centrifuged at $6750 \times g$ for 1 min. Then the bacterial precipitate was washed three times with PBS (0.01 M, pH 7.2) and the suspension concentration was diluted to 10^{5-6} CFU/mL. An equal volume of FAM286 was mixed with the bacterial solution so that the final concentration of it was $1 \times$ MBC, $2 \times$ MBC and $4 \times$ MBC, aliquots of sterile

PBS were used as negative control. The samples were incubated at 37 °C for 2 h. Centrifuge 100 μ L and discard the supernatant. 100 μ L of PI (30 μ mol/L) dye was added, mixed well and incubated at 4 °C for 15 min protected from light. After the staining was completed, the samples were washed twice with PBS. The fluorescence intensity was measured using a multimode plate reader. The excitation wavelength was set at 535 nm and the emission wavelength was set at 570–750 nm (Liu et al., 2015). And the 1 \times MBC FAM286 concentration group was selected for fluorescence microscopy based on the above experimental results (Ning et al., 2021).

The bacterial fluids of *S. aureus* at the logarithmic growth stage were washed three times with PBS. The concentration of the bacterial suspension was diluted to 10⁵⁻⁶ CFU/mL. Equal volumes of FAM286 were mixed with the bacterial fluids to make the final concentration of 1 \times MBC and 2 \times MBC. PBS was used as the negative control, while kanamycin and ϵ -polylysine were used as positive controls. According to the instructions of the Annexin V-FITC/PI cell apoptosis detection kit, it was tested at 1 h and 2 h, respectively. 100 μ L of the sample and 5 μ L of Annexin V/FITC mixed well at room temperature in the dark for 5 min. Subsequently, 5 μ L of PI and 400 μ L of PBS were added to the sample, and flow cytometry detection was immediately performed (Liu et al., 2022).

2.4.4. Effect on biofilm

The effect of FAM286 on the ability of *S. aureus* biofilm formation was assessed using the crystal violet quantification method as previously described (Song et al., 2020). 100 μ L of *S. aureus* bacterial solution at a concentration of 10⁵⁻⁶ CFU/mL was added to 96-well plates. The FAM286 solution was diluted using NB medium to a final concentration of 1/16 \times MBC, 1/8 \times MBC, 1/4 \times MBC, 1/2 \times MBC, 1 \times MBC. Subsequently, 100 μ L of these different concentrations of FAM286 were added to the corresponding wells of the 96-well plate. The same volume of NB medium was used as a control group. The 96-well plates were incubated at 37 °C for 72 h. To evaluate the biofilm degradation effects, biofilms were allowed to form and mature for 24 h at 37 °C. Then, the bacterial suspension was removed and replaced with FAM286 and incubated for 2 h. Then, the medium and floating cells were removed, and the plates were washed twice with PBS (0.01 M, pH 7.2), and then 200 μ L of methanol solution was added to fix the plates for 10 min. After removing the methanol, the plates were allowed to stand until evaporation, and then 200 μ L of 1% crystalline violet solution was added to them, and then they were placed in the dark and stained at room temperature for 15 min. Then washed with PBS until no color flowed out. The crystalline violet was extracted using a mixture of 10% acetic acid and 30% methanol, and the absorbance value was measured using an enzyme counter at a wavelength of 600 nm.

The 2D structure of FAM286 was predicted by the software ultra v12.0 Chemdraw and converted into a 3D structure and hydrogenated with ultra v14.0 ChemBio3D. The crystal structure of *S. aureus* biofilm protein was downloaded from the Protein Structure Data Bank (<https://www.pdb.org/>). Molecular docking analysis was performed by the software Autodock Vina 1.1.2. using the FAM286 as the ligand and the target macromolecule as the receptor. Docking interaction sites were set and the complex with the lowest binding energy was selected as the most favorable binding mode and visualized using Pymol 2.0, as described by Li et al. (2023).

2.4.5. Interaction between FAM286 and bacteria DNA

DNA of *S. aureus* was extracted using a bacterial genomic DNA kit, and the resulting DNA was determined by ultra-micro spectrophotometer to determine the concentration and the purity of the extracted DNA by using 260 nm and 280 nm optical density ratio. Different concentrations of FAM286 were added so that the peptide/DNA mass ratios were 1:1, 5:4, 5:3, 5:2, 5:1, 10:1, 20:1, respectively. The equal amounts of sterile PBS (0.01 M, pH 7.2) were used as the control group, kanamycin and ϵ -polylysine as positive controls. After mixing, the samples

were incubated at 37 °C for 2 h. 8 μ L of each sample was mixed with 2 μ L of 10 \times DNA loading buffer and subjected to electrophoresis on a 1% agarose gel. The migration of DNA was detected by imaging using a gel imager with 20 s exposure to a 320 nm UV lamp (Yuan et al., 2022).

The DNA was diluted to 50 μ g/mL with 1 \times TE buffer. 5 μ L of DNA solution and 10 μ L EB (100 μ g/mL) solution were added to each well of a 96-well plate, mixed well and incubated at 37 °C for 10 min in the dark. Subsequently, 50 μ L of FAM286 at different concentrations were added, resulting in final concentrations of 1/2 \times MBC, 1 \times MBC, 2 \times MBC, 4 \times MBC and 8 \times MBC. Additionally, 50 μ L of PBS (0.01 M, pH 7.2) was added to serve as the control group. After mixing, the samples were incubated for 30 min at 37 °C protected from light. The fluorescence intensity was measured using a multimode plate reader at an excitation wavelengths of 535 nm and an emission wavelength range of 570 nm–710 nm (Hou et al., 2019).

2.5. Statistical analysis

All experiments were conducted in triplicate, and the results were analyzed with SPSS software (version 22.0 for Windows) with a one-way ANOVA test. Significance was indicated at $p < 0.05$.

3. Results and discussion

3.1. Screening potential AMPs from *L. crocea*

Ten peptide sequences were identified from *L. crocea* using UPLC-MS (Table 1). The peptide sequences, which ranged in length from 7 to 19 amino acids and had molecular weights ranging from 746 to 2245 Da, were recorded. The charges and hydrophobicity of the peptide sequences were calculated using the online software APD3. Their net charges ranged from -3 to $+2$, and hydrophobicity rates ranged from 17% to 64%.

One of the peptides, No.7 (PRQVCPYAVISFHFK), was derived from the *L. crocea* TASOR protein (Ao et al., 2015), named FAM286, with a molecular weight of 1791 Da, 2 net positive charges, 47% hydrophobicity, which are typical AMPs characteristics (net charge $+2$ to $+9$, hydrophobicity $>30\%$). TASOR is a multi-interacting protein that affects genomic stability, involved in DNA/RNA binding and transcriptional regulation, and plays an important role in immunity (Gresakova et al., 2021). Studies have found increased expression of TASOR has been found in cells infected by external microorganisms, suggesting that the up-regulated TASOR protein may be involved in the body's immune response in some way, such as by degrading its own proteins to produce AMPs (Zhang et al., 2023).

3.2. Antimicrobial activity of the peptide FAM286

The bactericidal effect of the peptide FAM286 against *S. aureus* was verified using a plate coating method. As shown in Table 2, the MBC of the peptide FAM286 against *S. aureus* was 3.9 μ g/mL. Among the selected common antibiotics, kanamycin exhibited better antimicrobial activity against *S. aureus* with the MBC of 62.5 μ g/mL. *S. aureus* demonstrated resistance to enrofloxacin, amoxicillin, and florfenicol, with MBCs of the three antibiotics exceeding 1000 μ g/mL. Nisin showed the MBC of 500 μ g/mL, while ϵ -polylysine showed good bactericidal activity against *S. aureus* with the MBC of 7.8 μ g/mL. Compared with the four antibiotics and the two food preservatives, the antimicrobial activity of the peptide FAM286 could be up to 2–250 times higher. It has the potential to replace them as a novel type of food preservative. In most cases, AMPs exhibit superior antimicrobial activity compared to traditional antibiotics, primarily due to their differing mechanisms of action. Bacteria can easily develop antibiotic resistance through mutation because the target site category of traditional antibiotic action is very limited (Guo et al., 2020). The most common mechanism of AMPs is the direct disruptive effect on bacterial cell membranes, then cross cell

Table 1
Predicted potential antimicrobial peptides isolated from *Larimichthys crocea*.

No.	Peptide sequences	MW (Da)	Hydrophobic Ratio (%)	Net charge	Protein	Start position
1	AGRTSAGK	746	25	+2	RNA helicase	364
2	CGGAEAGSCCTSK	1102	33	0	Tenascin-X	123
3	FSVDEEYPDLSLHNNHMAK	2245	32	-3	Creatine kinase	13
4	GLAFILGAEGVKEQSQR	1802	41	0	Brefeldin A-inhibited guanine nucleotide-exchange protein 3	162
5	INFDAFLPMLK	1307	64	0	Myosin light chain 3, skeletal muscle isoform	67
6	LDSVDQTPVQSKR	1472	23	0	Phosducin	60
7	PRQVCPYAVISFHFK	1791	47	+2	TASOR	286
8	REGTALR	801	29	+1	F-box/WD repeat-containing protein 7	68
9	SETIEEKIKGYR	1452	17	0	Cytochrome C oxidase subunit	2
10	VPTPNVSVVDLTVR	1495	43	0	Glyceraldehyde-3-phosphate dehydrogenase	233

Table 2
Antimicrobial activity of FAM286, antibiotics and food preservatives against *S. aureus*.

Antimicrobial agents	MBC ($\mu\text{g/mL}$)	
Antimicrobial peptide	FAM286	3.9
Antibiotics	Kanamycin	62.5
	Enrofloxacin	1000
	Amoxicillin	3500
	Florfenicol	5500
Food Preservative	ϵ -Polylysine	7.8
	Nisin	500

membranes to interfere with the synthesis of nucleic acids, proteins or other components (Li et al., 2022). AMPs have low risk of bacterial resistance due to their non-specific antimicrobial mechanism and the presence of multiple targets in the cell (Luo and Song, 2021).

The antimicrobial activity of the FAM286 against *S. aureus* was further analyzed by time-kill curve (Fig. 1). The number of bacteria treated with the FAM286 was significantly reduced as time progressed. Different concentrations of FAM286 exhibited significant inhibitory effects on *S. aureus* after 0.5 h. Specifically, the bactericidal number of $4 \times \text{MBC}$ could reach 100%, and the $2 \times \text{MBC}$ and $1 \times \text{MBC}$ FAM286 also completely inhibited the growth of bacteria after 1 h and 1.5 h, respectively. With the prolongation of time, the bactericidal effect did not weaken. In contrast, 62.5 $\mu\text{g/mL}$ of kanamycin and 7.8 $\mu\text{g/mL}$ of ϵ -polylysine showed lower antimicrobial efficiencies, which required higher antimicrobial concentrations and treatment for 2.5 h and 3.0 h, respectively, to completely kill bacteria.

Factors such as the source, charge and hydrophobicity of AMPs collectively determine their antimicrobial activity. The aquatic environment exposes fish to numerous pathogens, and fish-derived AMPs have good antimicrobial effects on pathogenic bacteria in the water, with the minimum bactericidal concentration mostly at the micromolar

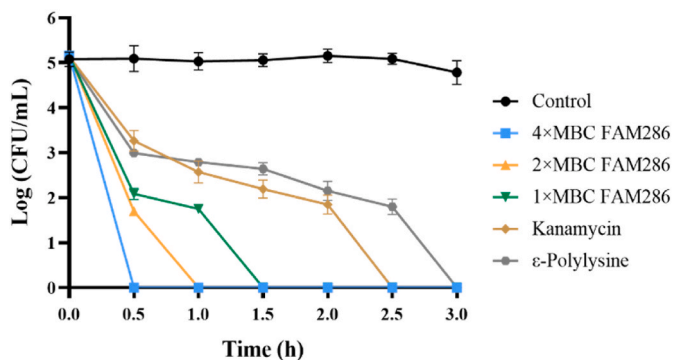


Fig. 1. Time-kill curve of FAM286 against *S. aureus*. $1 \times \text{MBC}$ FAM286 was 3.9 $\mu\text{g/mL}$, PBS buffer (0.01 M, pH 7.2) as control group. Kanamycin was 62.5 $\mu\text{g/mL}$ and ϵ -polylysine was 7.8 $\mu\text{g/mL}$.

level (Houyvet et al., 2021). The minimum inhibitory concentration of hemoglobin-derived AMP LCH4 against *S. aureus* identified from *L. crocea* was 12.5 $\mu\text{g/mL}$, reducing the bacterial count by 98.8% after 8 h. Similarly, the MIC of *L. crocea* whey acidic protein-derived peptide LCWAP against *S. aureus* was 15.6 $\mu\text{g/mL}$, with a bacterial reduction of 83.1% after 3 h of treatment and 99.2% after 5 h of treatment (Yang et al., 2020b). Since the bacterial cell membrane surface is typically negatively charged, positively charged AMPs can bind to it through electrostatic interactions, with their hydrophobic ends inserted into the phospholipid bilayer, leading to cell death by inducing the formation of barrel-stave model, carpet model, and toroidal model (Yan et al., 2021). The proportion of hydrophobic amino acids usually determines the strength of the peptide's attachment to the cell membrane. And peptides with high hydrophobicity tend to stay on the membrane for a longer period of time, allowing them to play a more effective role in disrupting the cell membrane (Bin Hafeez et al., 2021).

3.3. Effect on *S. aureus* cell membrane of FAM286

3.3.1. Effect of the cell membrane permeability by FAM286

The cell membrane is the main barrier against leakage of cellular contents. The binding and permeation of AMPs to the bacterial cell membrane typically constitute the initial phase of their interaction (Hollmann et al., 2018). In the measurement of nucleic acid leakage (Fig. 2a), the amount of nucleic acid released from the blank control group remained stable, indicating no significant nucleic acid leakage and unchanged permeability of the bacterial cell membrane. Different concentrations of FAM286 treatment group at 2 h OD₂₆₀ increased significantly, indicating that the bacteria have undergone nucleic acid leakage phenomenon. The result showed a concentration-dependent relationship, which is attributed to the increased permeability of the cell membrane following treatment with FAM286. In the measurement of protein leakage (Fig. 2b), the OD₂₈₀ of the FAM286-treated group showed a significant upward trend when time was prolonged. The result indicated that the permeability of the bacterial cell membrane increased and intracellular protein flowed out. This result is basically consistent with the time-kill curve.

No significant leakage of nucleic acids or proteins occurred in the kanamycin and ϵ -polylysine-treated group, which was related to the time of action of antimicrobial activity and its antimicrobial mechanism. Kanamycin belongs to aminoglycoside antibiotics, and its main inhibition mechanism involves binding irreversibly to bacterial ribosomal 30S subunit, inducing gene coding errors and preventing bacterial protein synthesis (Wohlgemuth et al., 2021). Since its target of action is not the cell membrane, kanamycin has no significant effect on the permeability of the cell membrane, and thus does not cause obvious leakage of nucleic acids and proteins. Studies have shown that ϵ -polylysine neutralizes the negative charge of the cell membrane on the surface of gram-positive bacteria, leading to disruption of the cell membrane. However, these studies have failed to show that it induces a decrease in the permeability

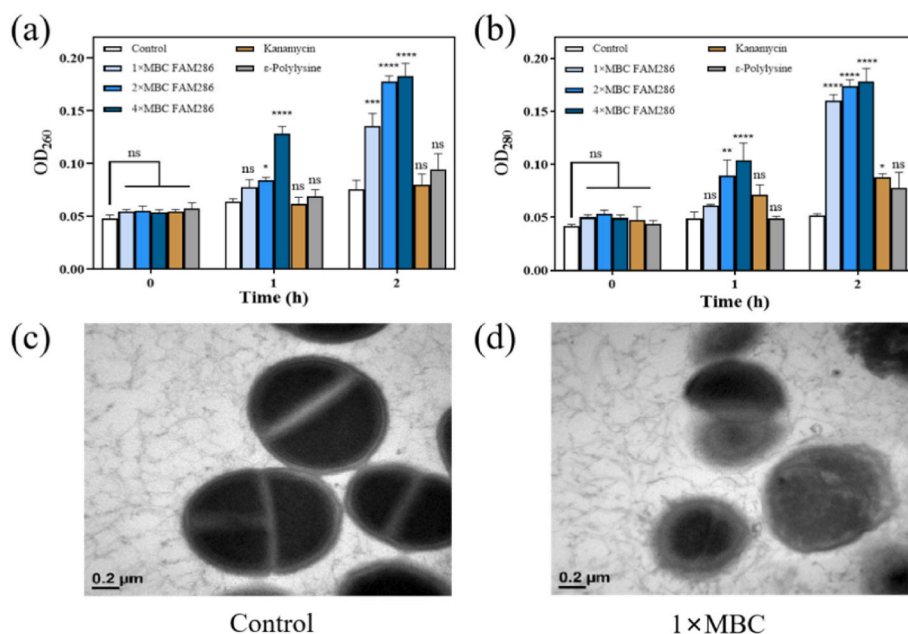


Fig. 2. Effect on cell membrane permeability. (a) Determination of FAM286 on the release of nucleic acid. (b) Determination of FAM286 on the release of protein. $1 \times$ MBC FAM286 was $3.9 \mu\text{g}/\text{mL}$, PBS buffer (0.01 M , $\text{pH } 7.2$) as control group. Kanamycin at $62.5 \mu\text{g}/\text{mL}$ and ϵ -polylysine at $7.8 \mu\text{g}/\text{mL}$. (c) TEM images of untreated *S. aureus* and treated with FAM286 for 2 h.

of the cell membrane leading to leakage of intracellular material (Lin et al., 2018). The results indicate that the FAM286 has a broader mechanism of action on the cell membrane, which can increase the permeability of the cell membrane of *S. aureus*, causing the leakage of intra-membrane substances into the extracellular space, ultimately inducing bacterial death.

3.3.2. Morphology changes induced by FAM286 in *S. aureus* cell membrane

Further we used transmission electron microscopy to observe the morphological changes in bacteria treated with FAM286. The bacteria in the control group had regular cell morphology as well as uniformly distributed intact and smooth cell membranes and showed dense internal organization (Fig. 2c). After 2 h of treatment with FAM286, the cell membrane of *S. aureus* was observably ruptured and severely deformed. The cytoplasmic density was reduced and unevenly distributed, and leakage of cytoplasmic material could be seen around the cells (Fig. 2d). This is attributed to the attractive interaction between the positive charge of FAM286 and the negative charge of the bacterial membrane, which tightly wraps FAM286 around the bacteria. It was shown that FAM286 has a damaging effect on the cell membrane and internal structure of *S. aureus*, corroborating the experimental results that indicate an increase in cell membrane permeability. It has been shown that AMPs can target and disrupt bacterial cell membranes, causing deformation and rupture, including pore formation, loss of hyphae, and cytoplasmic efflux (Chen et al., 2023).

3.3.3. Determination of the cell membrane integrity

PI, a fluorescein that cannot intact cell membrane, serves as a fluorescent marker. When the cell membrane is sufficiently damaged, PI can penetrate into the cell through the defective cell membrane, bind to intracellular DNA and emit a red fluorescence at a specific excitation wavelength (Zhang et al., 2018). Therefore, the degree of cell damage can be determined based on the magnitude of fluorescence intensity. In Fig. 3a, all treatment groups of PI exhibited maximum fluorescence intensity at an emission wavelength of 650 nm . Notably, the fluorescence intensity of FAM286 alone and when combined with PI was very low. The fluorescence intensity of *S. aureus* treated with $1 \times$ MBC, $2 \times$ MBC, and $4 \times$ MBC FAM286 was significantly higher than that of the blank

control group. The fluorescence intensity increased with the concentration of FAM286, which indicated that different concentrations of FAM286 caused damage to the cell membrane of *S. aureus* and disrupted their integrity. The degree of the cell membrane damage was positively correlated with the concentration of FAM286 in a concentration-dependent manner. AMPs could cause cell lysis by disrupting the integrity of the cell membrane or by interacting with the membrane to form transient pores, which in turn transport the AMPs into the cell and act on intracellular material (Last and Miranker, 2013). This experiment further verified that the FAM286 could damage to the cell membrane of *S. aureus*, leading to the death of the bacteria. Based on its mechanism of physically destroying cell membrane integrity, FAM286 is expected to be a promising new type of bacteriostatic agent for sustainable development.

3.3.4. Effect of FAM286 on cell membrane integrity by fluorescence microscopy

Fig. 3b shows the fluorescence microscope images of PI-stained *S. aureus* cells in the control group and samples treated with FAM286, respectively. In the control group, few red light spots appeared in the vast majority of *S. aureus* organisms, indicating that the cell membranes of the cells were still in an intact state so that the PI dye could not enter. After treatment with FAM286, the *S. aureus* showed strong fluorescence, indicating severe damage to the bacterial cell membranes and an obvious aggregation phenomenon. This indicates that FAM286 may affect the charge distribution on the cell surface by altering the content and distribution of surface substances, leading to cell depolarization and membrane damage. These changes weaken the hydrophobic interactions between cells, promote cell aggregation, and ultimately disrupt the integrity of bacterial cell membranes, thereby adversely affecting cell viability. (Li et al., 2023; Yi et al., 2020).

3.3.5. Flow cytometric analysis of FAM286 against *S. aureus*

The results of Annexin-V FITC/PI double staining assay showed that the ratio of viable cells in the blank group was 89.65% after 2 h (Fig. 3c). When *S. aureus* cells were treated with the FAM286 at $1 \times$ MBC for 1 h, the viable cells decreased to 38.58% , and 50.36% of the cells entering late apoptosis. After 2 h of treatment, only 3.76% of the viable cells

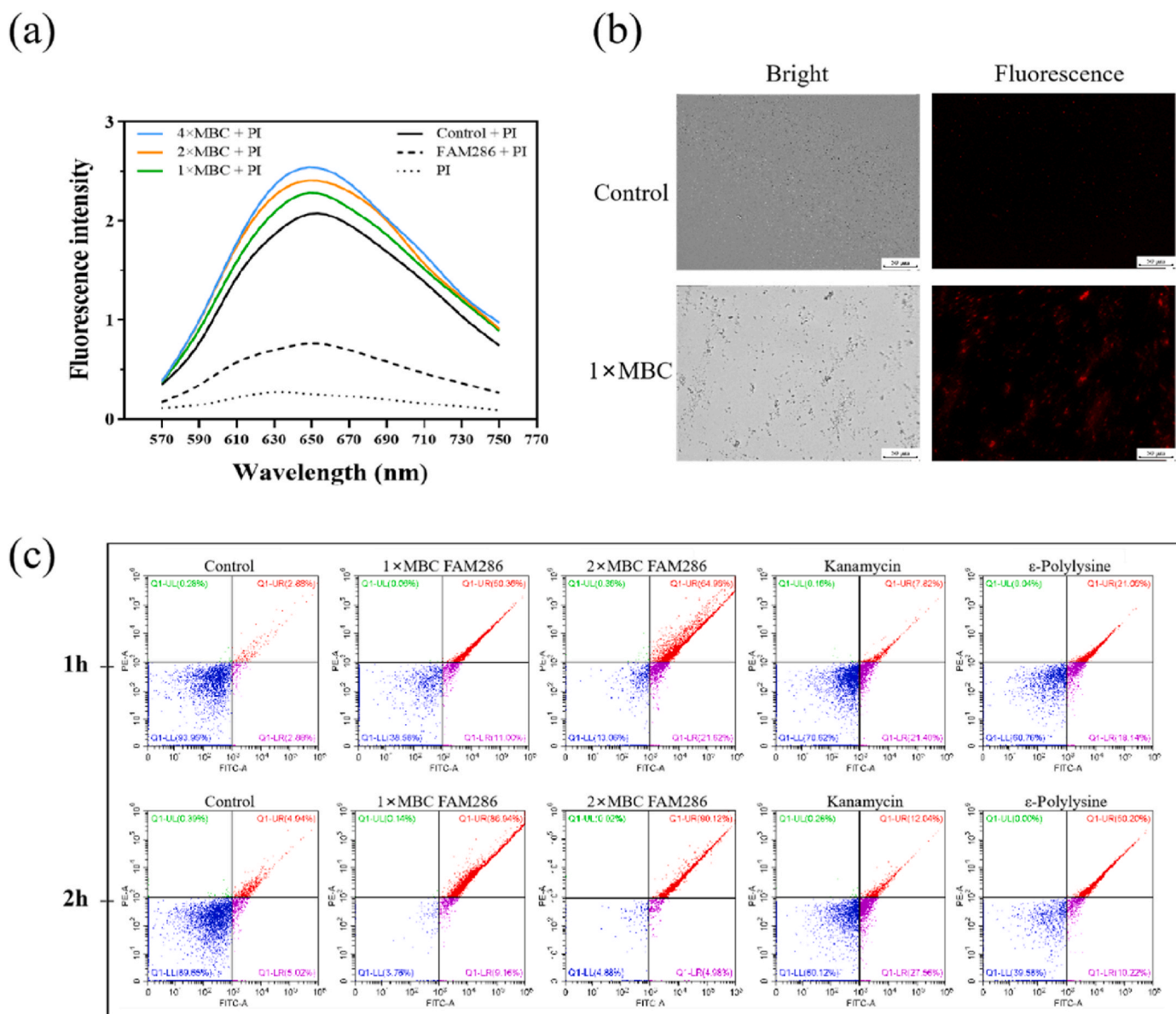


Fig. 3. Effect on cell membrane integrity. (a) The fluorescence intensity of PI treated with FAM286. 1 × MBC was 3.9 μg/mL, PBS buffer (0.01 M, pH 7.2) as control group, PI concentration is 30 μmol/L. The fluorescence spectra were measured from 570 to 750 nm. (b) Fluorescence microscope images of *S. aureus* treated with FAM286. 1 × MBC was 3.9 μg/mL. (c) Flow cytometry to determine the integrity of bacterial cell membrane. 1 × MBC FAM286 was 3.9 μg/mL, PBS buffer (0.01 M, pH 7.2) as control group. Kanamycin at 62.5 μg/mL and ε-polylysine at 7.8 μg/mL.

survived, and the late apoptotic cells increased to 86.94%. When the bacteria were treated with 2 × MBC FAM286, the viable cells decreased from 13.06% at 1 h to 4.88% at 2 h. The late apoptotic cells increased from 64.96% to 90.12%, primarily due to cells transitioning from early to late apoptosis. In contrast, the effect of ε-polylysine on apoptosis was weak, with 39.58% of viable cells remaining after 2 h of treatment. The effect of kanamycin on apoptosis was less obvious. The FAM286 caused a large amount of apoptosis of *S. aureus* within 2 h. Its impact on disrupting the *S. aureus* cell membrane was much higher than that of kanamycin and ε-polylysine, which depended on its highly efficient bacterial inhibitory activity and physical membrane-breaking inhibitory mechanism. Studies have found that antimicrobial peptides can participate in cellular immune responses, control cell apoptosis, regulate the host immune system, and alleviate inflammation caused by pathogens (Dai et al., 2018). These results indicate that the antimicrobial peptide FAM286 can induce apoptosis in *Staphylococcus aureus* and lead to programmed cell death.

3.4. Effect of FAM286 on biofilm formation

3.4.1. Inhibition of biofilm formation and removal of mature biofilm by FAM286

Bacterial biofilm is the adhesion of cells to living and non-living surfaces via extracellular polymeric molecules, and biofilm formation is widely recognized as a significant factor in the persistence of bacterial contamination of foods (Guo et al., 2023). In this experiment, crystal violet staining was used to quantify the biofilm and assess the effect of FAM286 on *S. aureus* biofilm formation. The biofilm of the control group strains was intact, whereas biofilm formation was reduced in the presence of FAM286 (Fig. 4a). The rate of *S. aureus* biofilm formation was gradually decreased with the increase of the concentration of FAM286, which indicated that FAM286 was able to inhibit the formation of *S. aureus* biofilm significantly. And the rate of inhibition was positively correlated with the concentration of FAM286. Non-bactericidal concentrations of FAM286 significantly inhibited the formation of *S. aureus*

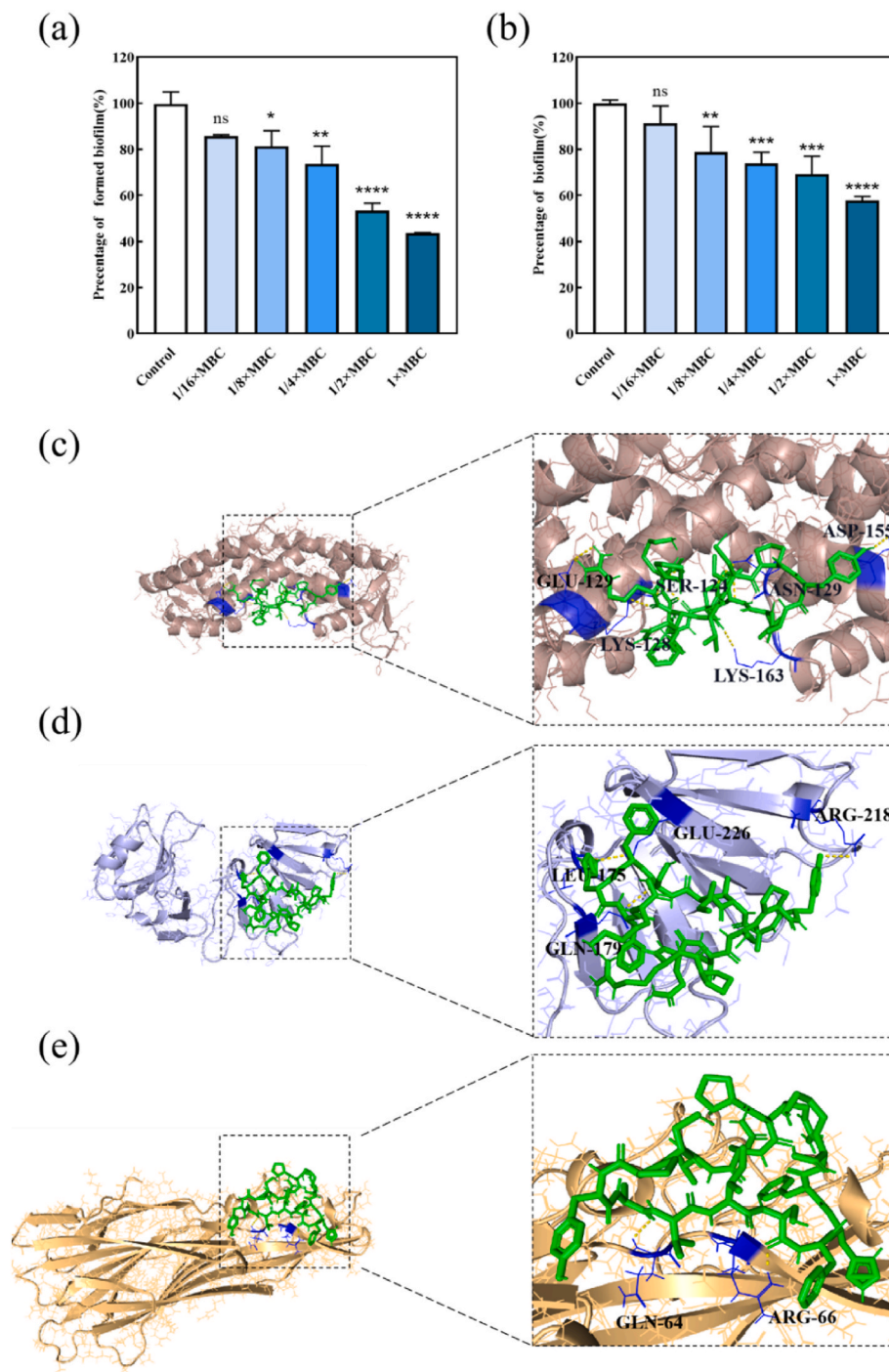


Fig. 4. Effect of FAM286 on biofilm. (a) Inhibitory effect of FAM286 on biofilm formation. (b) Clearance effect of FAM286 on biofilm formed. $1 \times \text{MBC}$ was $3.9 \mu\text{g}/\text{mL}$, PBS buffer (0.01 M, pH 7.2) as control group. * $P < 0.05$, ** $P < 0.01$, *** $P < 0.005$, **** $P < 0.001$. (c) Molecular docking of FAM286 with *S. aureus* SarA. FAM286 is shown in green and the backbone of the macromolecule (SarA) is shown as a brown cartoon. Residues in the protein are shown in blue. The yellow dots indicate hydrogen bonds. (d) Molecular docking of FAM286 with *S. aureus* AgrA. FAM286 is shown in green and the backbone of the macromolecule (AgrA) is shown as a purple cartoon. Residues in the protein are shown in blue. The yellow dots indicate hydrogen bonds. (e) Molecular docking of FAM286 with *S. aureus* Hld. FAM286 is shown in green and the backbone of the macromolecule (Hld) is shown as an orange cartoon. Residues in the protein are shown in blue. The yellow dots indicate hydrogen bonds.

biofilm.

In the experiment of removing mature biofilms, although non-bactericidal concentrations of FAM286 can remove some biofilms (Fig. 4b), but it is more difficult than the inhibition of biofilm formation. The focus should be on avoiding initial cell adhesion, accumulation, and late biofilm formation.

3.4.2. Molecular docking analysis of FAM286 binding to biofilm proteins

As described previously, FAM286 can effectively inhibit the formation of *S. aureus* biofilm. In this study, we modeled the binding of FAM286 to biofilm-associated proteins and the related sites of action by molecular docking.

The binding site of the FAM286 to *S. aureus* biofilm proteins was

further validated by molecular docking. The FAM286 formed a total of six hydrogen bonds with *S. aureus* SarA at chain a: SER-124, LYS-128, and GLU-129, and chain b: ASN-129, ASP-155, and LYS-163, which occurred as an insertion binding between the protein SarA bilayers at a minimum binding energy of -6.2 kcal/mol (Fig. 4c). The FAM286 has a docking binding energy of -5.6 kcal/mol to *S. aureus* AgrA and forms four hydrogen bonds at LEU-175, GLN-179, ARG-218, and GLU-226 (Fig. 4d). The docking binding energy of the FAM286 to *S. aureus* Hld was -5.6 kcal/mol, with the formation of 2 hydrogen bonds at GLN-64, ARG-66 (Fig. 4e).

SarA is an important virulence gene regulator that regulates the expression of about 120 genes involved in numerous physiological processes related to pathogenicity of *S. aureus*, such as biofilm synthesis and drug resistance (Li et al., 2016). AgrA is one of the two-component regulatory systems of bacteria that exhibit dual regulation of their virulence expression. Proteins associated with host cell adhesion and resistance to host defenses regulate the growth of bacterial populations until they are able to respond to attacks by host defenses (Leonard et al., 2012). α -HL, a β -barrel pore-forming toxin expressed by *S. aureus*, is able to form transmembrane β -barrel heptamer channels self-assembling on host cell membranes, attacking the cell membranes by extruding the lipid bilayer to form a hydrophilic transmembrane channel, leading to host cell lysis or death (Sugawara et al., 2015). The docking affinities of the FAM286 with each target protein were less than 0 kcal/mol, suggesting that FAM286 can bind to proteins spontaneously, exerting bacteriostatic and biofilm inhibitory activities.

3.5. Effect of FAM286 on bacterial DNA

3.5.1. Binding of FAM286 to *S. aureus* genomic DNA by agarose gel electrophoresis

In addition to disrupting bacterial cell membranes, AMPs can cause rapid cell death by binding to genomic DNA. The binding of FAM286 to *S. aureus* genomic DNA was analyzed using agarose gel electrophoresis (Fig. 5a). The results of the experiment showed that the genomic DNA of the control group was located in lane (a) and showed clear and bright DNA bands in the electropherogram. In lanes (b-c), there was no significant difference in band brightness compared to the blank group, and there was no blocked DNA in the spotted wells, indicating that FAM286 has no effect on DNA under these conditions. In lanes (d-h), DNA migration was affected by FAM286, resulting in DNA blocked in the spotted sample wells. As the concentration of FAM286 increases, the DNA is blocked entirely in the spot sample wells lane (e), at which point

the FAM286 to DNA mass ratio is 5:2. When the mass ratio continues to increase, the genomic DNA is still in the blocked state, at this time, the amount of sample visible in the spotted wells gradually decreased. When the mass ratio is 20:1, no sample remains visible in the spot wells, as shown in lane (h), indicating that the DNA has undergone cleavage. ϵ -polylysine was able to cleave genomic DNA completely across all tested mass ratios (Fig. 5b), and its ability to interact with DNA in vitro was superior to that of FAM286. In contrast, Fig. 5c shows the binding of kanamycin to genomic DNA. No samples were blocked in the spot wells and the brightness of the bands in different lanes was approximately the same, indicating that kanamycin at this mass ratio could not bind to genomic DNA. Complete DNA has a bright band in the gel, and the brightness of the bright band of broken DNA will decrease. The lower the brightness, the higher the cutting rate (Wang et al., 2023). This indicates that the antimicrobial peptide FAM286 can not only bind to DNA, but when the mass ratio is large enough ($>10/1$), FAM286 can cleave DNA, causing DNA fragmentation.

Gel blocking experiments showed that FAM286 has a strong binding ability to bacterial genomic DNA. The formation of this complex results in alterations in the relative molecular mass and charge of the DNA, causing a certain lag phenomenon in the electrophoretic mobility of the complex compared to that of free DNA fragments. The extent of this damage is positively correlated with its ratio.

3.5.2. Competitive binding of FAM286 and EB with *S. aureus* genomic DNA

EB is a fluorescent dye with a high affinity for binding to DNA. When embedded between the base pairs of double-stranded DNA with high affinity, the fluorescence intensity is greatly enhanced (Galindo-Murillo and Cheatham, 2021). The fluorescence intensity of DNA-EB complexes treated with FAM286 tended to decrease, where $8 \times$ MBC acting on the EB-DNA complex resulted in a substantial decrease in the fluorescence intensity of the system (Fig. 5d). These results indicate that FAM286 binds to the genomic DNA of *S. aureus*, causing the EB molecule inserted into the bacterial DNA to be replaced by FAM286. This result suggests that FAM286 has a stronger binding affinity than EB and binds to DNA through a nested insertion of base pairs. The fluorescence intensity did not change significantly at $1 \times$ MBC and $2 \times$ MBC, indicating that FAM286 binds to DNA in a similar proportion within this concentration range, potentially interfering with the binding of EB to DNA. However, compared to the control group, a significant decrease in fluorescence intensity was observed in all experimental groups, even at $1/2 \times$ MBC, indicating that FAM286 binds to a high proportion of DNA, which may affect the normal replication of DNA and inhibit the growth and reproduction of the organism. Similarly, the AMP CLFchimera exerts its antimicrobial activity after binding to DNA, when the hydrogen bond between the two DNA chains begins to break from one of the ends (Pirkhezranian et al., 2020). The AMP CA-TAT can interact with DNA through a tiny groove binding mode and target DNA to exert antimicrobial activity (Lv et al., 2018).

4. Conclusions

The AMP FAM286, identified from *L. crocea* TASOR protein, showed significant antimicrobial effect on *S. aureus*. The antimicrobial activity was dose and time-dependent, with a minimum bactericidal concentration of $3.9 \mu\text{g/mL}$, and completely killed the bacteria within 1.5 h. FAM286 can act on the cell membrane of bacteria to change its permeability, leading to a large amount of leakage of nucleic acids and proteins in the content, and destroying the integrity of the membrane, causing cell aggregation, and causing the cell to enter the apoptotic stage. At non-bactericidal concentrations. Additionally, molecular docking simulations were performed to investigate the binding of FAM286 with biofilm-associated proteins SarA, AgrA, and Hld. FAM286 could enter into the cell interior and bind to bacterial DNA in an embedded manner, disrupting the DNA structure and leading to the death of the bacterium. This study demonstrates that FAM286, derived

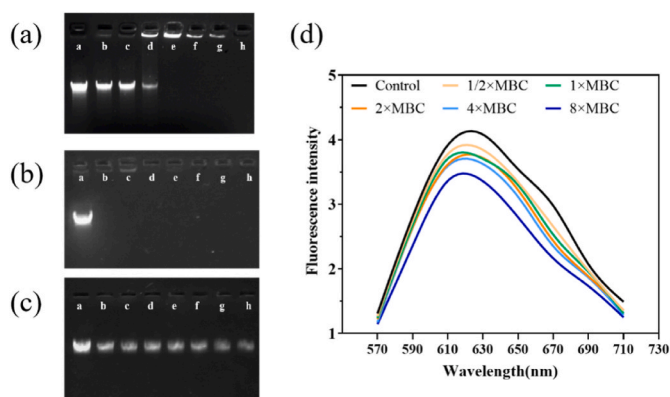


Fig. 5. Interaction between FAM286 and bacteria DNA. (a) Gel retardation analysis of *S. aureus* DNA treated with FAM286, (b) treated with ϵ -polylysine, (c) treated with kanamycin. Lane a: control. Lane b-h: FAM286/DNA weight ratios of 1:1, 5:4, 5:3, 5:2, 5:1, 10:1, 20:1, respectively. (d) Competitive binding of FAM286 and EB with *S. aureus* genomic DNA. $1 \times$ MBC was $3.9 \mu\text{g/mL}$. PBS buffer (0.01 M, pH 7.2) as control group. The fluorescence spectra were measured from 570 to 710 nm.

from the TASOR protein of *L. crocea*, exerts its antimicrobial effect on *S. aureus* through a multi-targeted antimicrobial mechanism, which provided a theoretical basis for its use as a natural bacteriostatic agent.

CRedit authorship contribution statement

Ritian Jin: Project administration, Formal analysis, Writing – original draft. **Guanglei Wei:** Visualization, Data curation. **Rong Lin:** Data curation. **Wenfeng Lin:** Methodology. **Jude Juventus Aweya:** Software, Validation. **Duo Liang:** Investigation. **Wuyin Weng:** Software. **Shen Yang:** Supervision, Resources, Writing – review & editing.

Funding

This work was supported by National Key R&D Program of China (2023YFD2100605), Natural Science Foundation of Fujian Province of China (2023J01775), and Fujian Provincial Oceanic and Fisheries Bureau, China (FJHYF-L-2023-17).

Declaration of competing interest

The authors declared that they have no conflicts of interest to this work. We declare that we do not have any commercial or associative interest that represents a conflict of interest in connection with the work submitted.

Data availability

Data will be made available on request.

References

- Ao, J., Mu, Y., Xiang, L.-X., Fan, D., Feng, M., Zhang, S., Shi, Q., Zhu, L.-Y., Li, T., Ding, Y., Nie, L., Li, Q., Dong, W., Jiang, L., Sun, B., Zhang, X., Li, M., Zhang, H.-Q., Xie, S., Zhu, Y., Jiang, X., Wang, X., Mu, P., Chen, W., Yue, Z., Wang, Z., Wang, J., Shao, J.-Z., Chen, X., 2015. Genome sequencing of the perciform fish *Larimichthys crocea* provides insights into molecular and genetic mechanisms of stress adaptation. *PLoS Genet.* 11, e1005118. <https://doi.org/10.1371/journal.pgen.1005118>.
- Ashrafudoulla, M., Mizan, M.F.R., Ha, A.J., Park, S.H., Ha, S.-D., 2020. Antibacterial and antibiofilm mechanism of eugenol against antibiotic resistance *Vibrio parahaemolyticus*. *Food Microbiol.* 91, 103500. <https://doi.org/10.1016/j.fm.2020.103500>.
- Bencardino, D., Amagliani, G., Brandi, G., 2021. Carriage of *Staphylococcus aureus* among food handlers: an ongoing challenge in public health. *Food Control* 130, 108362. <https://doi.org/10.1016/j.foodcont.2021.108362>.
- Bin Hafeez, A., Jiang, X., Bergen, P.J., Zhu, Y., 2021. Antimicrobial peptides: an update on classifications and databases. *Int. J. Mol. Sci.* 22, 11691. <https://doi.org/10.3390/ijms222111691>.
- Browne, K., Chakraborty, S., Chen, R., Willcox, M.D., Black, D.S., Walsh, W.R., Kumar, N., 2020. A new era of antibiotics: the clinical potential of antimicrobial peptides. *Int. J. Mol. Sci.* 21, 7047. <https://doi.org/10.3390/ijms21197047>.
- Chen, M., Lin, N., Liu, X., Tang, X., Wang, Z., Zhang, D., 2023. A novel antimicrobial peptide screened by a *Bacillus subtilis* expression system, derived from *Larimichthys crocea* Ferritin H, exerting bactericidal and parasiticidal activities. *Front. Immunol.* 14, 1168517. <https://doi.org/10.3389/fimmu.2023.1168517>.
- Dai, M., Pan, P., Li, H., Liu, S., Zhang, L., Song, C., Li, Y., Li, Q., Mao, Z., Long, Y., Su, X., Hu, C., 2018. The antimicrobial cathelicidin peptide hLF(1-11) attenuates alveolar macrophage pyroptosis induced by *Acinetobacter baumannii* in vivo. *Exp. Cell Res.* 364, 95–103. <https://doi.org/10.1016/j.yexcr.2018.01.035>.
- Erickson, M.C., Doyle, M.P., 2017. The challenges of eliminating or substituting antimicrobial preservatives in foods. *Annu. Rev. Food Sci. Technol.* 8, 371–390. <https://doi.org/10.1146/annurev-food-030216-025952>.
- Galindo-Murillo, R., Cheatham, T.E., 2021. Ethidium bromide interactions with DNA: an exploration of a classic DNA–ligand complex with unbiased molecular dynamics simulations. *Nucleic Acids Res.* 49, 3735–3747. <https://doi.org/10.1093/nar/gkab143>.
- Gresakova, V., Novosadova, V., Prochazkova, M., Prochazka, J., Sedlacek, R., 2021. Dual role of Fam208a during zygotic cleavage and early embryonic development. *Exp. Cell Res.* 406, 112723. <https://doi.org/10.1016/j.yexcr.2021.112723>.
- Guo, N., Bai, X., Shen, Y., Zhang, T., 2023. Target-based screening for natural products against *Staphylococcus aureus* biofilms. *Crit. Rev. Food Sci. Nutr.* 63, 2216–2230. <https://doi.org/10.1080/10408398.2021.1972280>.
- Guo, Y., Song, G., Sun, M., Wang, J., Wang, Y., 2020. Prevalence and therapies of antibiotic-resistance in *Staphylococcus aureus*. *Front. Cell. Infect. Microbiol.* 10. <https://doi.org/10.3389/fcimb.2020.00107>.
- Hollmann, A., Martinez, M., Maturana, P., Semorile, L.C., Maffia, P.C., 2018. Antimicrobial peptides: interaction with model and biological membranes and synergism with chemical antibiotics. *Front. Chem.* 6, 204. <https://doi.org/10.3389/fchem.2018.00204>.
- Hou, X., Feng, C., Li, S., Luo, Q., Shen, G., Wu, H., Li, M., Liu, X., Chen, A., Ye, M., Zhang, Z., 2019. Mechanism of antimicrobial peptide NP-6 from Sichuan pepper seeds against *E. coli* and effects of different environmental factors on its activity. *Appl. Microbiol. Biotechnol.* 103, 6593–6604. <https://doi.org/10.1007/s00253-019-09981-y>.
- Houyvet, B., Bouchon-Navaro, Y., Bouchon, C., Corre, E., Zatylny-Gaudin, C., 2021. Marine transcriptomics analysis for the identification of new antimicrobial peptides. *Mar. Drugs* 19, 490. <https://doi.org/10.3390/md19090490>.
- Kumar, Y., Kaur, I., Mishra, S., 2023. Foodborne disease symptoms, diagnostics, and predictions using artificial intelligence-based learning approaches: a systematic review. *Arch. Comput. Methods Eng.* 1–26. <https://doi.org/10.1007/s11831-023-09991-0>.
- Larsen, J., Stegger, M., Andersen, P.S., Petersen, A., Larsen, A.R., Westh, H., Agersø, Y., Fetsch, A., Kraushaar, B., Käsbohrer, A., Schwarz, S., Cuny, C., Witte, W., Butaye, P., Denis, O., Haenni, M., Madec, J.-Y., Jouy, E., Laurent, F., Battisti, A., Franco, A., Alba, P., Mammìna, C., Pantosti, A., Monaco, M., Wagenaar, J.A., De Boer, E., Van Duikeren, E., Heck, M., Domínguez, L., Torres, C., Zarazaga, M., Price, L.B., Skov, R. L., 2016. Evidence for human adaptation and foodborne transmission of livestock-associated methicillin-resistant *Staphylococcus aureus*: table 1. *Clin. Infect. Dis.* 63, 1349–1352. <https://doi.org/10.1093/cid/ciw532>.
- Last, N.B., Miranker, A.D., 2013. Common mechanism unites membrane poration by amyloid and antimicrobial peptides. *Proc. Natl. Acad. Sci. U.S.A.* 110, 6382–6387. <https://doi.org/10.1073/pnas.1219059110>.
- Leonard, P.G., Bezar, I.F., Sidote, D.J., Stock, A.M., 2012. Identification of a hydrophobic cleft in the LytTR domain of AgrA as a locus for small molecule interactions that inhibit DNA binding. *Biochemistry* 51, 10035–10043. <https://doi.org/10.1021/bi3011785>.
- Li, H.-L., Chen, Y.-N., Cai, J., Liao, T., Zu, X.-Y., 2023. Identification, screening and antibacterial mechanism analysis of novel antimicrobial peptides from sturgeon (*Acipenser ruthenus*) spermary. *Mar. Drugs* 21, 386. <https://doi.org/10.3390/md21070386>.
- Li, K., Li, W., Chen, Xiaojuan, Luo, T., Mu, Y., Chen, Xinhua, 2021. Molecular and functional identification of a β -defensin homolog in large yellow croaker (*Larimichthys crocea*). *J. Fish. Dis.* 44, 391–400. <https://doi.org/10.1111/jfd.13324>.
- Li, L., Cheung, A., Bayer, A.S., Chen, L., Abdelhady, W., Kreiswirth, B.N., Yeaman, M.R., Xiong, Y.Q., 2016. The global regulon *sarA* regulates β -lactam antibiotic resistance in methicillin-resistant *Staphylococcus aureus* in vitro and in endovascular infections. *J. Infect. Dis.* 214, 1421–1429. <https://doi.org/10.1093/infdis/jiw386>.
- Li, S., Wang, Y., Xue, Z., Jia, Y., Li, R., He, C., Chen, H., 2021. The structure-mechanism relationship and mode of actions of antimicrobial peptides: a review. *Trends Food Sci. Technol.* 109, 103–115. <https://doi.org/10.1016/j.tifs.2021.01.005>.
- Li, X., Zuo, S., Wang, B., Zhang, K., Wang, Y., 2022. Antimicrobial mechanisms and clinical application prospects of antimicrobial peptides. *Molecules* 27, 2675. <https://doi.org/10.3390/molecules27092675>.
- Lin, L., Gu, Y., Li, C., Vittayapadung, S., Cui, H., 2018. Antibacterial mechanism of ϵ -Poly-L-lysine against *Listeria monocytogenes* and its application on cheese. *Food Control* 91, 76–84. <https://doi.org/10.1016/j.foodcont.2018.03.025>.
- Liu, S., Aweya, J.J., Zheng, L., Zheng, Z., Huang, H., Wang, F., Yao, D., Ou, T., Zhang, Y., 2022. LvHemB1, a novel cationic antimicrobial peptide derived from the hemocyanin of *Litopenaeus vannamei*, induces cancer cell death by targeting mitochondrial voltage-dependent anion channel 1. *Cell Biol. Toxicol.* 38, 87–110. <https://doi.org/10.1007/s10565-021-09588-y>.
- Liu, H., Pei, H., Han, Z., Feng, G., Li, D., 2015. The antimicrobial effects and synergistic antibacterial mechanism of the combination of ϵ -Polylysine and nisin against *Bacillus subtilis*. *Food Control* 47, 444–450. <https://doi.org/10.1016/j.foodcont.2014.07.050>.
- Liu, X., Hu, Y.-Z., Pan, Y.-R., Liu, J., Jiang, Y.-B., Zhang, Y.-A., Zhang, X.-J., 2023. Comparative study on antibacterial characteristics of the multiple liver expressed antimicrobial peptides (LEAPs) in teleost fish. *Front. Immunol.* 14, 1128138. <https://doi.org/10.3389/fimmu.2023.1128138>.
- Liu, X., Kang, L., Liu, W., Lou, B., Wu, C., Jiang, L., 2017. Molecular characterization and expression analysis of the large yellow croaker (*Larimichthys crocea*) chemokine receptors CXCR2, CXCR3, and CXCR4 after bacterial and poly I:C challenge. *Fish Shellfish Immunol.* 70, 228–239. <https://doi.org/10.1016/j.fsi.2017.08.029>.
- Luo, Y., Song, Y., 2021. Mechanism of antimicrobial peptides: antimicrobial, anti-inflammatory and antibiofilm activities. *Int. J. Math. Stat.* 22, 11401. <https://doi.org/10.3390/ijms222111401>.
- Lv, M., Wang, M., Lu, K., Duan, B., Zhao, Y., 2018. Non-covalent interaction between CA-TAT and calf thymus DNA: deciphering the binding mode by in vitro studies. *Int. J. Biol. Macromol.* 114, 1354–1360. <https://doi.org/10.1016/j.jbiomac.2017.11.158>.
- Ning, H.-Q., Lin, H., Wang, J.-X., 2021. Synergistic effects of endolysin Lysqdpv001 and ϵ -poly-L-lysine in controlling *Vibrio parahaemolyticus* and its biofilms. *Int. J. Food Microbiol.* 343, 109112. <https://doi.org/10.1016/j.ijfoodmicro.2021.109112>.
- Pirkhezranian, Z., Tahmoospour, M., Daura, X., Monhemi, H., Sekhavati, M.H., 2020. Interaction of camel Lactoferrin derived peptides with DNA: a molecular dynamics study. *BMC Genom.* 21, 60. <https://doi.org/10.1186/s12864-020-6458-7>.
- Song, Y.J., Yu, H.H., Kim, Y.J., Lee, N.-K., Paik, H.-D., 2020. The use of papain for the removal of biofilms formed by pathogenic *Staphylococcus aureus* and *Campylobacter jejuni*. *Lebensm. Wiss. Technol.* 127, 109383. <https://doi.org/10.1016/j.lwt.2020.109383>.

- Sugawara, T., Yamashita, D., Kato, K., Peng, Z., Ueda, J., Kaneko, J., Kamio, Y., Tanaka, Y., Yao, M., 2015. Structural basis for pore-forming mechanism of staphylococcal α -hemolysin. *Toxicon* 108, 226–231. <https://doi.org/10.1016/j.toxicon.2015.09.033>.
- Tkaczewska, J., 2020. Peptides and protein hydrolysates as food preservatives and bioactive components of edible films and coatings - a review. *Trends Food Sci. Technol.* 106, 298–311. <https://doi.org/10.1016/j.tifs.2020.10.022>.
- Tao, W., Li, W., Aweya, J., Lin, R., Jin, R., Liang, D., Ren, Z., Yang, S., 2025. *Bacillus subtilis* fermented shrimp waste isolated peptide, PVQ9, and its antimicrobial mechanism on four Gram-positive foodborne bacteria. *Food Microbiol.* 125, 104654. <https://doi.org/10.1016/j.fm.2024.104654>.
- Wan, Y., Yang, L., Li, Q., Wang, Xiaowen, Zhou, T., Chen, D., Li, L., Wang, Y., Wang, Xin, 2023. Stability and emetic activity of enterotoxin like X (SELX) with high carrier rate of food poisoning *Staphylococcus aureus*. *Int. J. Food Microbiol.* 404, 110352. <https://doi.org/10.1016/j.ijfoodmicro.2023.110352>.
- Wang, J., Su, B., Dunham, R.A., 2022. Genome-wide identification of catfish antimicrobial peptides: a new perspective to enhance fish disease resistance. *Rev. Aquacult.* 14, 2002–2022. <https://doi.org/10.1111/raq.12684>.
- Wang, W., Li, P., Huang, Q., Zhu, Q., He, S., Bing, W., Zhang, Z., 2023. Functionalized antibacterial peptide with DNA cleavage activity for enhanced bacterial disinfection. *Colloids Surf. B Biointerfaces* 228, 113412. <https://doi.org/10.1016/j.colsurfb.2023.113412>.
- Weng, Z., Zeng, F., Wang, M., Guo, S., Tang, Z., Itagaki, K., Lin, Y., Shen, X., Cao, Y., Duan, J., Wang, F., 2023. Antimicrobial activities of lavandulylated flavonoids in *Sophora flavences* against methicillin-resistant *Staphylococcus aureus* via membrane disruption. *J. Adv. Res.* S2090123223001236. <https://doi.org/10.1016/j.jare.2023.04.017>.
- Wohlgemuth, I., Garofalo, R., Samatova, E., Güneç, A.N., Lenz, C., Urlaub, H., Rodnina, M.V., 2021. Translation error clusters induced by aminoglycoside antibiotics. *Nat. Commun.* 12, 1830. <https://doi.org/10.1038/s41467-021-21942-6>.
- Wu, C., Zhang, D., Kan, M., Lv, Z., Zhu, A., Su, Y., Zhou, D., Zhang, J., Zhang, Z., Xu, M., Jiang, L., Guo, B., Wang, T., Chi, C., Mao, Y., Zhou, J., Yu, X., Wang, H., Weng, X., Jin, J.G., Ye, J., He, L., Liu, Y., 2014. The draft genome of the large yellow croaker reveals well-developed innate immunity. *Nat. Commun.* 5, 5227. <https://doi.org/10.1038/ncomms6227>.
- Yan, Y., Li, Y., Zhang, Z., Wang, X., Niu, Y., Zhang, S., Xu, W., Ren, C., 2021. Advances of peptides for antibacterial applications. *Colloids Surf. B Biointerfaces* 202, 111682. <https://doi.org/10.1016/j.colsurfb.2021.111682>.
- Yang, S., Dong, Y., Aweya, J., Li, J., Chen, X., Zhang, Y., Liu, G., 2020a. A hemoglobin-derived antimicrobial peptide, LCH4, from the large yellow croaker (*Larimichthys crocea*) with potential use as a food preservative. *LWT—Food Sci. Technol.* 131, 109656. <https://doi.org/10.1016/j.lwt.2020.109656>.
- Yang, S., Li, J., Aweya, J., Yuan, Z., Weng, W., Zhang, Y., Liu, G., 2020b. Antimicrobial mechanism of *Larimichthys crocea* whey acidic protein-derived peptide (LCWAP) against *Staphylococcus aureus* and its application in milk. *Int. J. Food Microbiol.* 335, 108891. <https://doi.org/10.1016/j.ijfoodmicro.2020.108891>.
- Yang, S., Huang, H., Aweya, J., Zheng, Z., Liu, G., Zhang, Y., 2021. PvHS9 is a novel in silico predicted antimicrobial peptide derived from hemocyanin of *Penaeus vannamei*. *Aquaculture* 530, 735926. <https://doi.org/10.1016/j.aquaculture.2020.735926>.
- Yang, S., Wang, M., Gao, J., Liu, J., Jin, R., Lin, R., Weng, W., Aweya, J.J., 2023. Sodium chloride augments the antibacterial activity of a novel penaeid shrimp-derived peptide (GPCR10) against halotolerant *Staphylococcus aureus*. *Lebensm. Wiss. Technol.* 184, 115096. <https://doi.org/10.1016/j.lwt.2023.115096>.
- Yi, L., Luo, L., Chen, J., Sun, H., Wang, X., Yi, Y., Lv, X., 2020. Cell wall and DNA damage of *Staphylococcus aureus* by bacteriocin BM1157. *Lebensm. Wiss. Technol.* 134, 109842. <https://doi.org/10.1016/j.lwt.2020.109842>.
- Yuan, Z., Aweya, J., Li, J., Wang, Z., Huang, S., Zheng, M., Shi, L., Deng, S., Yang, S., 2022. Synergistic antibacterial effects of low-intensity ultrasound and peptide LCMHC against *Staphylococcus aureus*. *Int. J. Food Microbiol.* 373, 109713. <https://doi.org/10.1016/j.ijfoodmicro.2022.109713>.
- Zhang, M., Sun, W., You, X., Xu, D., Wang, L., Yang, J., Li, E., He, S., 2023. LINE-1 repression in Epstein–Barr virus-associated gastric cancer through viral–host genome interaction. *Nucleic Acids Res.* 51, 4867–4880. <https://doi.org/10.1093/nar/gkad203>.
- Zhang, N., Fan, Y., Li, C., Wang, Q., Leksawasdi, N., Li, F., Wang, S., 2018. Cell permeability and nuclear DNA staining by propidium iodide in basidiomycetous yeasts. *Appl. Microbiol. Biotechnol.* 102, 4183–4191. <https://doi.org/10.1007/s00253-018-8906-8>.
- Zhang, Y., Lu, L., Li, C., Shao, G., Chen, X., 2021. Transcriptome analysis revealed multiple immune processes and energy metabolism pathways involved in the defense response of the large yellow croaker *Larimichthys crocea* against *Pseudomonas plecoglossicida*. *Comp. Biochem. Physiol. Genom. Proteonomics* 40, 100886. <https://doi.org/10.1016/j.cbd.2021.100886>.
- Zheng, L., Mao, Y., Wang, J., Chen, R., Su, Y., Hong, Yue-qun, Hong, Yu-jian, Hong, Yu-cong, 2018. Excavating differentially expressed antimicrobial peptides from transcriptome of *Larimichthys crocea* liver in response to *Cryptocaryon irritans*. *Fish Shellfish Immunol.* 75, 109–114. <https://doi.org/10.1016/j.fsi.2018.01.028>.